PRRL-77-CR-12

ERDA/JPL/954465-77/1
Distribution Category UC-63

SILICON SHEET GROWTH BY THE INVERTED STEPANOV TECHNIQUE

S. Berkman, G. W. Cullen, M. T. Duffy,
and K. M. Kim

RCA Laboratories
Princeton, New Jersey 08540

QUARTERLY REPORT NO. 4

March 1977

This work was performed for the Jet Propulsion Laboratory, California Institute of Technology, under NASA Contract NAS7-100 for the U. S. Energy Research and Development Administration, Division of Solar Energy.

The JPL Low-Cost Silicon Solar Array Project is funded by ERDA and forms part of the ERDA Photovoltaic Conversion Program to initiate a major effort toward the development of low-cost solar arrays.

Prepared Under Contract No. 954465 For
JET PROPULSION LABORATORY
CALIFORNIA INSTITUTE OF TECHNOLOGY
Pasadena, California 91103

PREFACE

This Quarterly Report No. 4, prepared by RCA Laboratories, Princeton, New Jersey 08540, describes work performed under Contract No. 954465 in the Process and Applied Materials Research Laboratory, P. Rappaport, Director. G. W. Cullen is the Group Head and the Project Supervisor. Major contributors to this quarterly report are S. Berkman, M. T. Duffy, and K. M. Kim. Others who participated in the research are H. E. Temple, R. E. Novak, and S. H. McFarlane.

The JPL Project Monitor is K. M. Koliwad.

TABLE OF CONTENTS

LIST OF ILLUSTRATIONS

SECTION I

SUMMARY

Chemically vapor deposited silicon nitride and silicon oxynitride (CVD-Si_3N_4 and CVD-SiO_xN_y, respectively) are being evaluated as the contact material for molten silicon in the ribbon growth configuration. Thin films of the contact material are deposited on substrates such as boron nitride (BN) and hot-pressed and reaction-sintered silicon nitride (RS-Si_3N_4). Preliminary evaluation of the reactivity of molten silicon with the CVD-Si_3N_4 and CVD-SiO_xN_y indicates that these materials are considerably more resistant to reaction with and/or dissolution in silicon than other materials examined to date. The SiO_xN_y appears to be more stable in contact with the molten silicon than the Si_3N_4. Of the various substrates examined, RS-Si_3N_4 is the most favored. There is a problem, however, in obtaining high-purity, reaction-sintered Si_3N_4.

Reaction-sintered Si_3N_4 and BN die materials used for the growth of silicon ribbon were coated with CVD-Si_3N_4. Various graphite substrates were coated with CVD-Si_3N_4 and CVD-SiO_xN_y and used in silicon sessile drop experiments to determine compatibility in thermal expansion properties between film and substrate. Among six graphite grades (from Ultra Carbon Corporation), substrates designated UT-8 were most compatible with both types of CVD coatings in the sessile drop tests.

Ribbon growth runs have been carried out using dies coated with the CVD-Si_3N_4. Stable growth of narrow ribbons has been achieved. The grown ribbons are typically 0.05 to 0.06 cm thick, 0.3 to 0.5 cm wide. Ribbon growth experiments are being conducted to establish a stable growth of wide ribbons, but the width decreases continually during growth. It is concluded that the instability is caused primarily by the unfavorable convex isotherm during seeding and growth, which is delineated by the shape of the striations on the ribbon surface. Efforts are in progress to improve the width, resistivity, and crystallinity by use of purer die components and by modifying the growth conditions.

~~The Mark II ribbon growth apparatus is being assembled.~~

SECTION II

INTRODUCTION

The inverted Stepanov program was originally started to provide shaped crystal growth by use of nonwetting dies as an alternative method to the conventional Stepanov [1] and edge-defined film-fed growth (EFG) or capillary action shaping technique (CAST) [2,3] processes. Figure 1 is a schematic representation of silicon ribbon growth in the inverted Stepanov configuration. Using this setup, die liner materials can readily be employed which have contact angles spanning those required for either EFG or Stepanov growth.

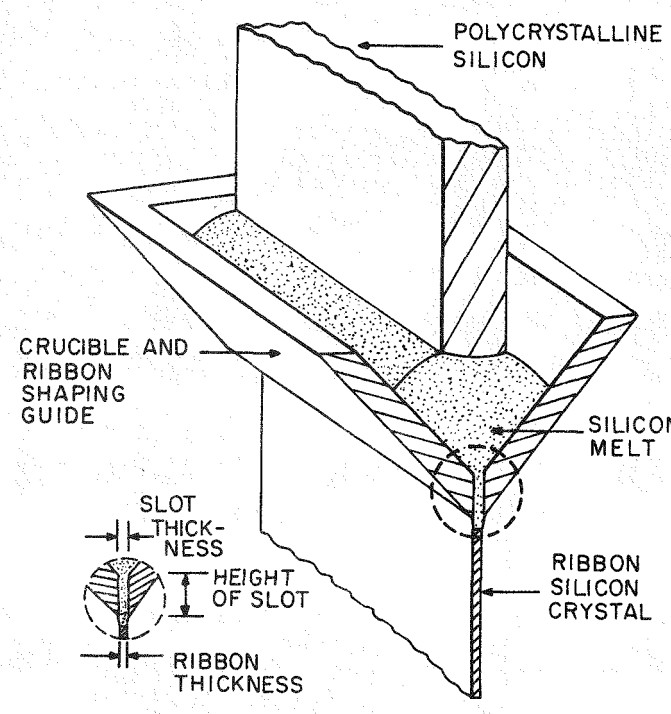

Figure 1. Schematic drawing of silicon ribbon growth by the inverted Stepanov technique (IST).

1. A. V. Stepanov et al., Bull. Acad. Sci. USSR, Phys. Series 33, 1826 (1969).
2. J. C. Schwartz, T. Surek, and B. Chalmers, J. Electronic Mat. 4, 255 (1975); H. E. Bates, F. H. Cooks, and A. I. Mlavsky, "Thick Film Silicon Growth Technique," NAS-100/JPL-953365, First Quarterly Progress Report, July 1972.
3. T. F. Ciszek, Mat. Res. Bull. 7, 731 (1972).

Fused silica dies (contact angle of 87°) were used during the initial phase of the inverted Stepanov program. We have found, however, that the applicability of fused silica is rather limited because of the hysteresis of the contact angle as the result of the formation and evolution of silicon monoxide at the interface between the silica die and the liquid silicon. The hysteresis prevented "pinning" the meniscus at the die edge to establish an effective meniscus shaping for the ribbon growth. Even though the growth instabilities associated with the hysteresis of the contact angle do not necessarily appear to be insurmountable, it was decided that more rapid progress (in light of the JPL time goals) would be achieved using die materials other than fused silica.

Silicon nitride (Si_3N_4) is currently being evaluated as the die material on this program. Si_3N_4 is deposited on substrate materials such as RS-Si_3N_4 and graphite. The graphites are chosen to match the thermal expansion coefficient of the nitride as closely as possible. The CVD-Si_3N_4 has a contact angle of 53°. Ribbon growth with dies coated with CVD-Si_3N_4 is described in this progress report.

SECTION III

PROGRESS AND TECHNICAL DISCUSSION

A. REACTIVITY OF THE MOLTEN SILICON WITH DIE MATERIALS COATED WITH CVD-Si_3N_4 AND CVD-SiO_xN_y

Die materials, such as RS-Si_3N_4, hot-pressed Si_3N_4, BN, and quartz have been coated with CVD-Si_3N_4 or CVD-SiO_xN_y. Of these, the CVD-Si_3N_4/RS-Si_3N_4 combination has been most frequently used in attempts to grow silicon ribbon; the CVD-Si_3N_4/BN combination has been used to a lesser extent. Figure 2(a) shows a photograph of a cross-section of a CVD-Si_3N_4/RS-Si_3N_4 die that has been used for pulling silicon ribbon. The photograph corresponds to an end-on view near the bottom of the die and shows the central solidified silicon column bounded by the CVD-Si_3N_4 layers and the shaped outer RS-Si_3N_4. The cut face was lapped and the silicon slightly etched to help provide contrast between the different regions. An enlarged view of one of the CVD-Si_3N_4 layers at the bottom of the die is shown in Fig. 2(b). Some chipping at the lower edge occurred during cutting. The CVD film remains continuous after about 2 h in contact with molten silicon. Similar dies have been reused for ribbon growth experiments without apparent dissolution of the CVD layer.

Experiments were conducted with CVD-Si_3N_4/RS-Si_3N_4 and CVD-SiO_xN_y/RS-Si_3N_4 composites, in which a molten silicon drop, 20° to 30°C above the melting point, was supported by the CVD coating for extended periods of time in a helium ambient. The samples were subsequently sectioned through the frozen silicon droplet and mounted in epoxy for lapping, etching, and profile examination. Figure 3(a) shows a photograph of a Si/CVD-Si_3N_4/RS-Si_3N_4 sectioned sample at the edge of the silicon drop, and Fig. 3(b) shows the profile toward the center of the drop. The heating time was 1 h at approximately 1440°C. The continuity of the film appears intact between the silicon and substrate and also around the edge of the substrate. Figures 4(a) and 4(b) show similar profiles for a sample heated at approximately 1450°C for 4 h. There is evidence of film fracture during the cutting operations in Fig. 4(a). The original

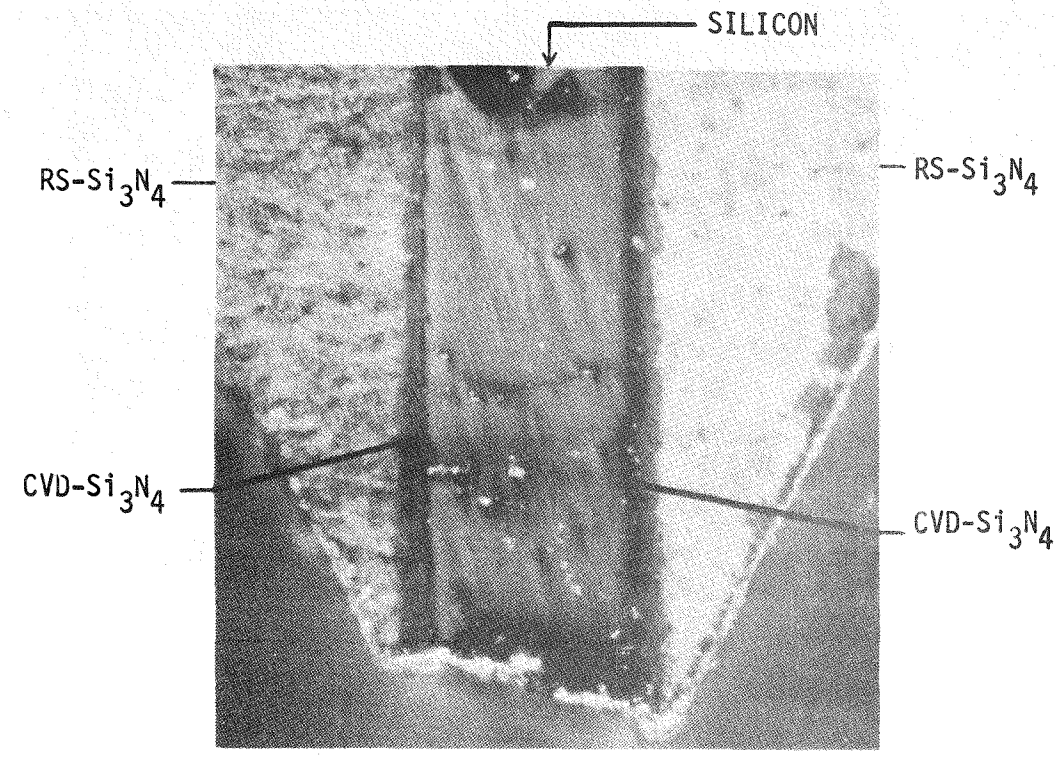

(a) ∿50X

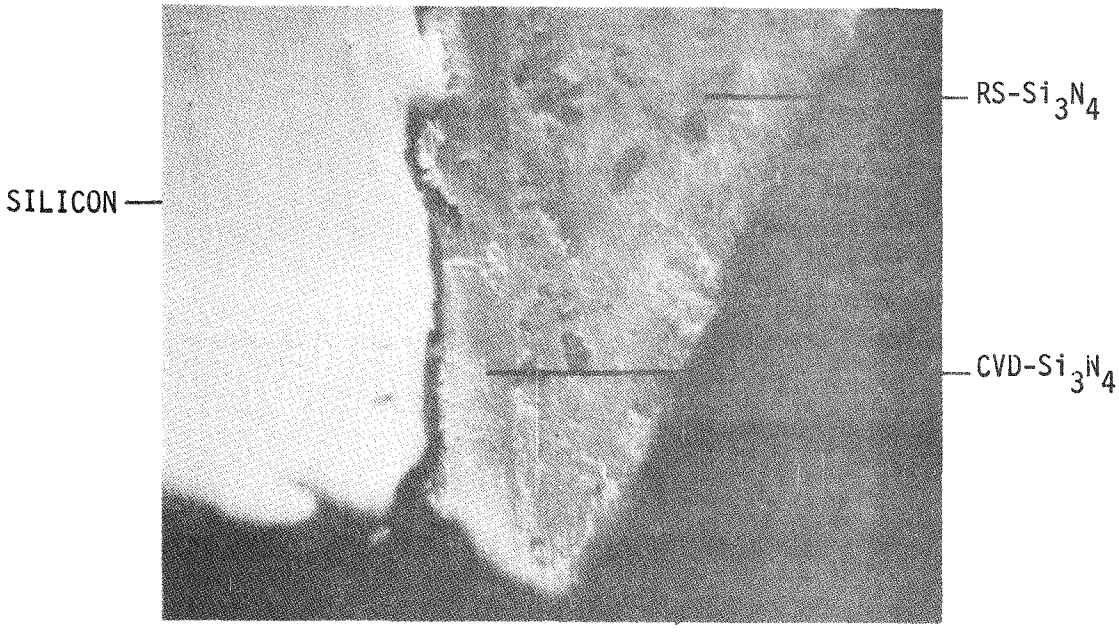

(b) ∿260X

Figure 2. Cross-sectional view of a silicon ribbon die showing (a) solidified silicon column bounded by CVD-Si_3N_4 and outer RS-Si_3N_4 shaped die and (b) enlarged view of CVD-Si_3N_4 layer. The die was maintained at liquid silicon temperatures for about 2 h.

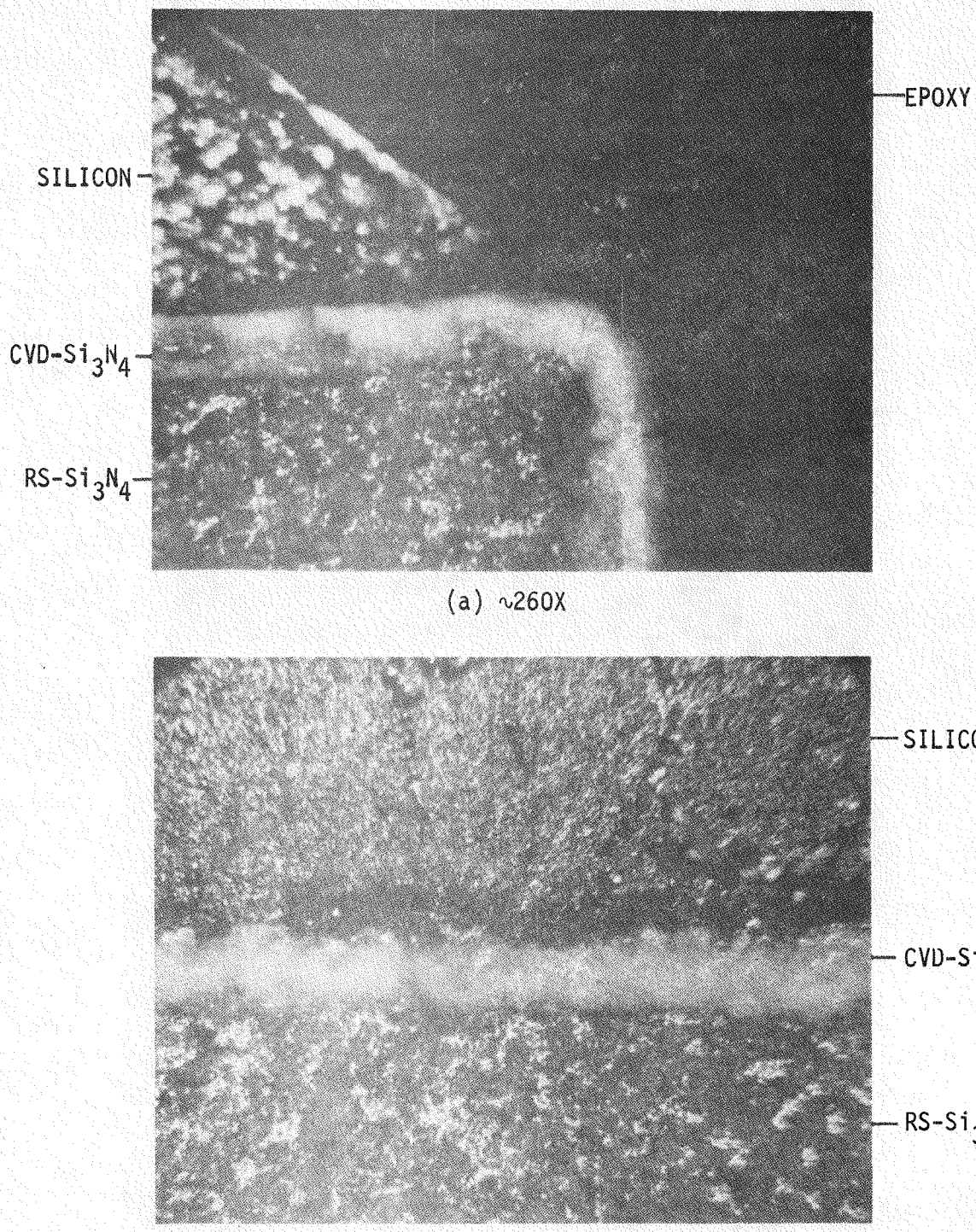

Figure 3. Photograph of a section of Si/CVD-Si_3N_4/RS-Si_3N_4 sample showing film continuity (a) near edge of silicon droplet and (b) under droplet after 1 h at 1440°C.

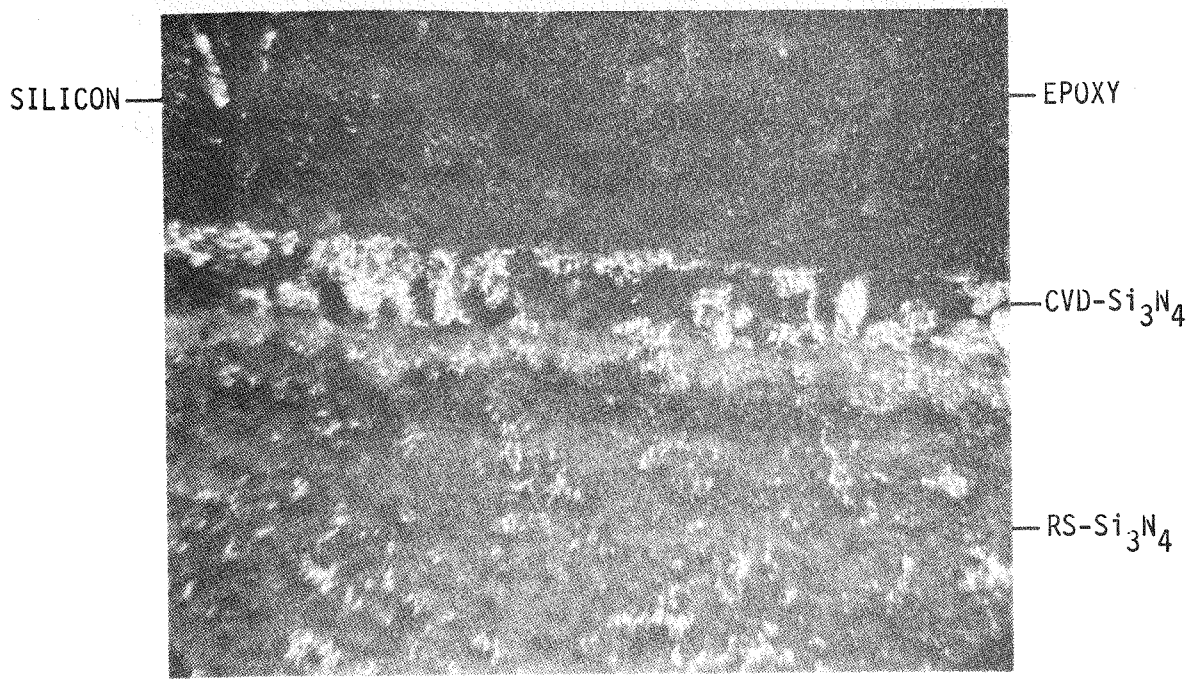

(a) ∿260X

(b) ∿260X

Figure 4. Photograph of a section Si/CVD-Si_3N_4/RS-Si_3N_4 sample showing film thickness continuity (a) near edge of silicon droplet and (b) under silicon droplet after 4 h at 1450°C. Some fracture of the CVD as a result of the cutting action is apparent.

thickness of the film appears unchanged, but the mechanical strength of the film has apparently deteriorated as evidenced by results of a scratch test on the CVD nitride layer after the silicon was etched off. Similar photographs for the case of a Si/CVD-SiO_xN_y/RS-Si_3N_4, heated simultaneously with the latter sample at 1450°C for 4 h, are shown in Figs. 5(a) and (b). Again film continuity is maintained, and, in this case, no deterioration in mechanical strength was observed from a scratch test performed after the silicon was etched off.

Other observations are as follows: when silicon is etched from the film/substrate composite, the area from which the silicon was removed has a brown color. Microscopic examination shows the presence of well-defined crystallites in a shallow surface brown coating. Two types of crystallites are apparent; elongated brown-colored needles and small dark crystallites. On CVD-Si_3N_4 surfaces, x-ray analysis has shown the presence of crystalline β-Si_3N_4 and β-SiC. On CVD-SiO_xN_y surfaces x-ray analysis has shown the presence of α-Si_3N_4, β-SiC, and a crystalline phase not identifiable at this time. It should be indicated that there has been some controversy about the composition of "α-Si_3N_4," as to whether it is a phase of Si_3N_4 or an oxynitride. The systems used here have contained graphite which could account for the formation of β-SiC by carbon transport if O_2 were present as an impurity in the gas stream. Likewise, β-Si_3N_4 could also be accounted for if N_2 were present in the gas stream. These are preliminary results with commercially available materials, and no effort has been made to control impurity content. We believe that impurity content in starting materials has a major impact on the compatibility of all contact materials in this program. For example, CVD-Si_3N_4 films on BN have shown greater reactivity with molten silicon than CVD-Si_3N_4 on RS-Si_3N_4 die materials. In turn, hot-pressed Si_3N_4 has provided a very poor substrate for CVD coatings with a large emission of impurities at liquid silicon temperatures. RS-Si_3N_4 also emits considerable amounts of impurities at these temperatures. Current efforts are directed toward realizing higher purities in the deposited layers and the substrates.

All of the dies used in the recent attempts to grow silicon ribbon were coated with CVD-Si_3N_4. The die substrate material was principally RS-Si_3N_4, and in a few cases BN. The CVD layers appear to remain continuous during the temperature cycle of the growth process.

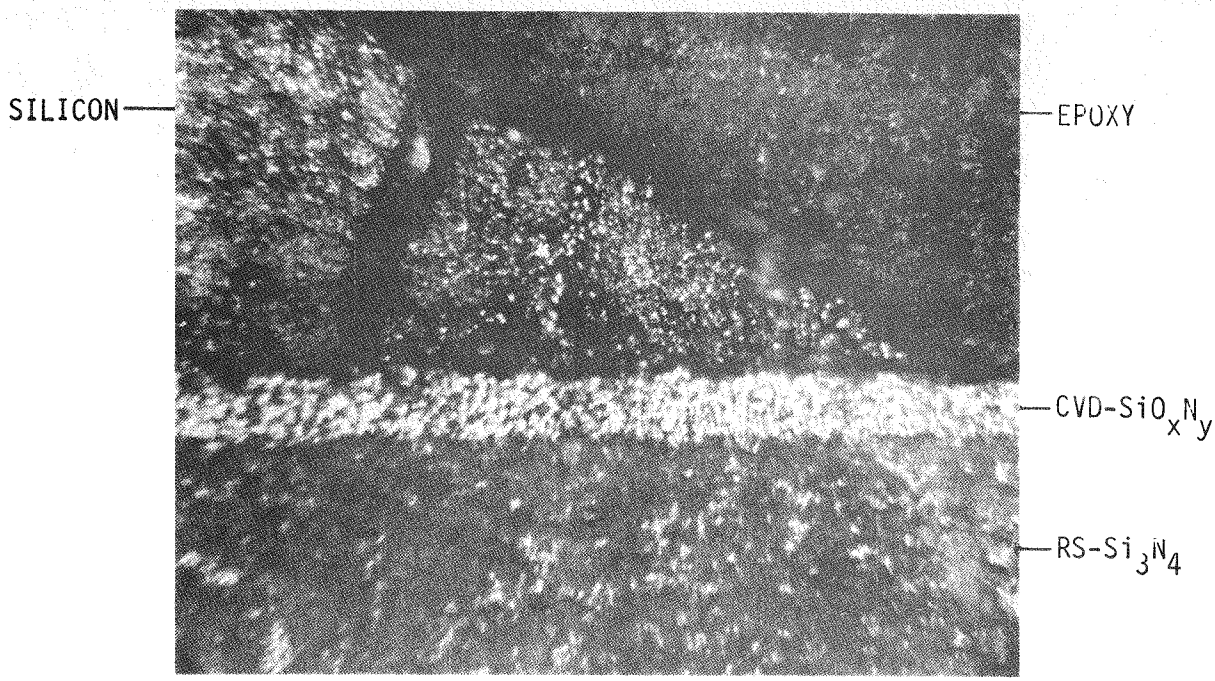

(a) ∿260X

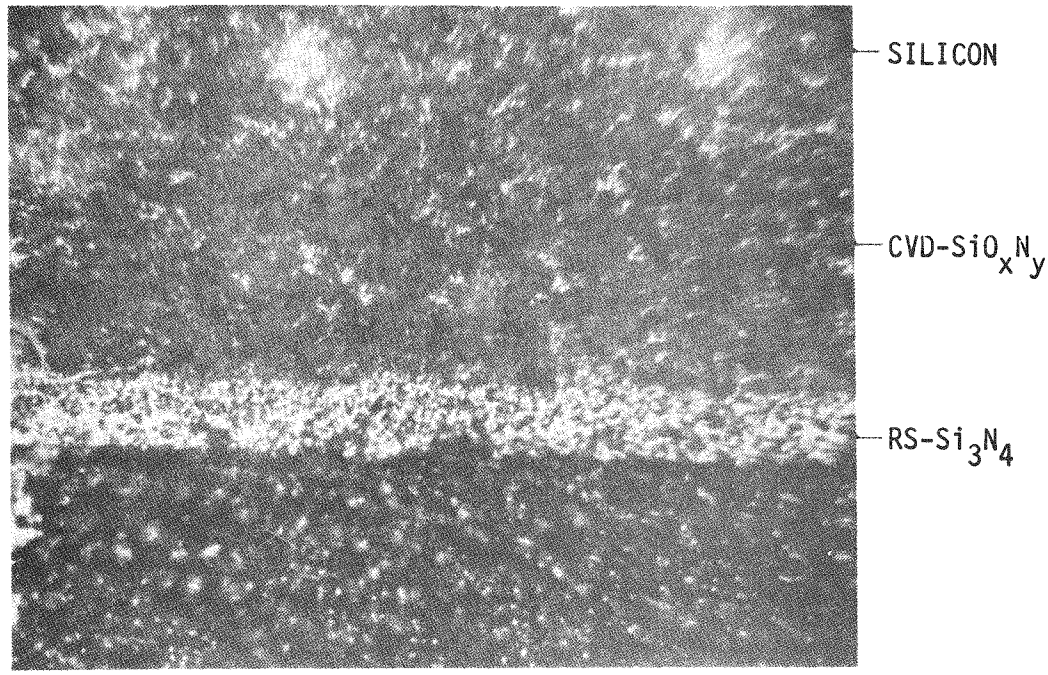

(b) ∿260X

Figure 5. Photograph of a sectioned Si/CVD-SiO$_x$N$_y$/RS-Si$_3$N$_4$ sample showing film thickness continuity (a) near edge of silicon droplet and (b) under silicon droplet after 4 h at 1450°C. No film fracture was observed.

In peripheral experiments various grades of graphite were coated with CVD-Si_3N_4 or SiO_xN_y and subjected to a silicon sessile drop test at 1450°C for 1 h. Figure 6(a) is a photograph is six Ultra Carbon* graphite samples, with corresponding designations, which has been coated with Si_3N_4. With the exception of UT-8, all samples show a mismatch in thermal expansion properties between the film and the substrate, leading to film cracking and absorption of the silicon droplet into the substrate. The curvature of the samples is apparent from the shadowing effect in the photograph. The Si_3N_4/UT-8 composite was only slightly curved and the film remained intact. The graphite substrates had a CVD coating on one side only.

Figure 6(b) shows a corresponding set of samples for CVD-SiO_xN_y with the substrates coated on both sides. Sample UT-8 was the least affected in this case also. All specimens remained flat because of the CVD layer on both sides. The film on UT-2-S, UT-6, and UT-6ST displayed some cracks when viewed microscopically. The cracking occurred during the cooling process since the silicon droplets remain on the composites.

B. IST SILICON RIBBON GROWTH USING CVD-Si_3N_4 COATED DIES

Silicon ribbon growth has been carried out in the inverted Stepanov configuration using the V-shaped crucible/die assembly coated with CVD-Si_3N_4. As the substrate material for the CVD coating, two kinds of Si_3N_4 were used, i.e., RS-Si_3N_4 and hot-pressed Si_3N_4 (Cerac, Inc., Milwaukee, WI). The purity of these substrate materials is low. Table 1 shows semi-quantitative emission spectrographic analyses of both kinds of Si_3N_4. Analysis of the CVD-Si_3N_4 and hot-pressed Si_3N_4 from a different source (Atomergic Chemical Co., Long Island, NY) is also given in Table 1. It is of interest to note that the CVD-Si_3N_4 is much purer than the other Si_3N_4; the purity of the CVD material can be further improved. The density of the substrate silicon nitrides was about 75% of the theoretical density, and thus relatively porous. Since the CVD layer conforms rather closely to the morphology of the substrate, the CVD-Si_3N_4 coating was not completely flat. Substrate materials of high purity and high density are therefore desirable for the improvement of the CVD coating.

*Ultra Corporation, Bay City, MI.

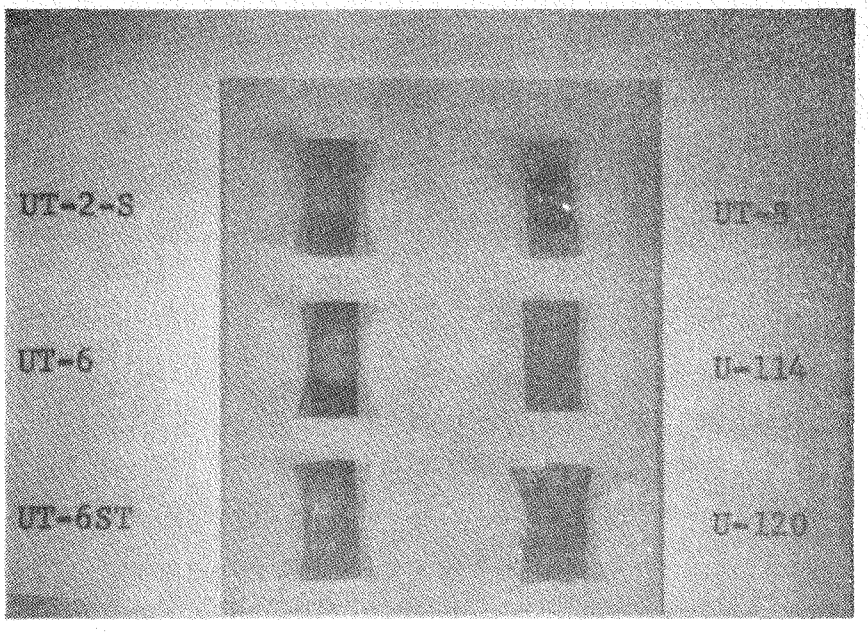

(a)

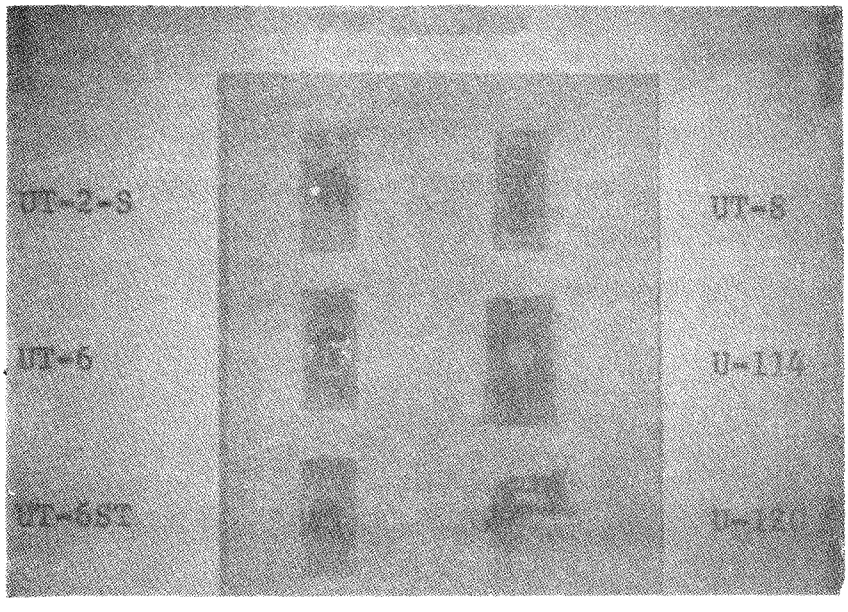

(b)

Figure 6. Silicon sessile drop test on (a) Si_3N_4/graphite composites, CVD coating on one side of each substrate and (b) SiO_xN_y/graphite composites, CVD coating on both sides of each substrate.

TABLE 1. EMISSION SPECTROGRAPHIC ANALYSIS OF VARIOUS SILICON NITRIDES (ppmw)

	Hot-Pressed (Atomergic)	Hot Pressed (Cerac)	Reaction Sintered (Cerac)	CVD Film
Cu	6-60	60-600	60-600	0.1-1
Ti	30-300	300-3000	300-3000	-
V	-	20-200	20-200	-
Ba	1-10	100-1000	10-100	-
B	15-150	60-600	6-60	10-100
Si	S	S	S	S
Mg	0.3%-3%	0.3%-3%	30-300	1-10
Mn	1-10	100-1000	100-1000	0.3-3
Cr	-	100-1000	60-600	-
Fe	30-3000	60-600	500-5000	0.3-3
Al	0.6%-6%	1%-10%	1%-100%	3-30
Be	-	3-30	0.6-6	-
Mo	-	3-30	30-300	-
Ca	30-300	600-6000	300-3000	-
Ni	3-30	60-600	100-1000	-

The die surfaces exposed to the liquid silicon during the ribbon growth were coated with from ∿25 to ∿100 μm of CVD-Si_3N_4. The hot-pressed Si_3N_4 has a second phase, and CVD-coated dies made of this material outgas severely at the ribbon growth temperature. On the other hand, RS-Si_3N_4 is single phase, and there is less outgassing during ribbon growth. Therefore, RS-Si_3N_4 is being employed as the CVD substrate material for the die. The size of the die slot opening was 0.05 x 2.5 cm and 0.3 cm high. Typically, the (110)[11$\bar{2}$] silicon seeds were 0.04 cm thick, 1.2 to 2.0 cm wide, and ∿5 cm long.

A number of thermal trimmers have been employed in the growth configuration (see Quarterly Report No. 3, Dec. 1976, p. 6 [4]). With a pyrolytic graphite plate trimmer, which is similar to the trimmer 1a, it has been possible to achieve a stable and sustained growth of narrow ribbons. Figure 7 shows two silicon ribbons, 0.05 to 0.06 cm thick and 0.3 to 0.5 cm wide, which have been grown with the CVD-coated Si_3N_4 die. The ribbon width is small compared with the width of the seed and the die aperture. The narrowing of the grown ribbon is considered to be the result of an unsatisfactory isotherm at the solid-liquid (s-ℓ) ribbon growth interface. Both ribbons in Fig. 7 were grown at a rate of 10 cm/h. By increasing the growth rate and decreasing the temperature, it has been possible to increase the ribbon width to some extent (see the right-hand section of the lower ribbon in Fig. 7).

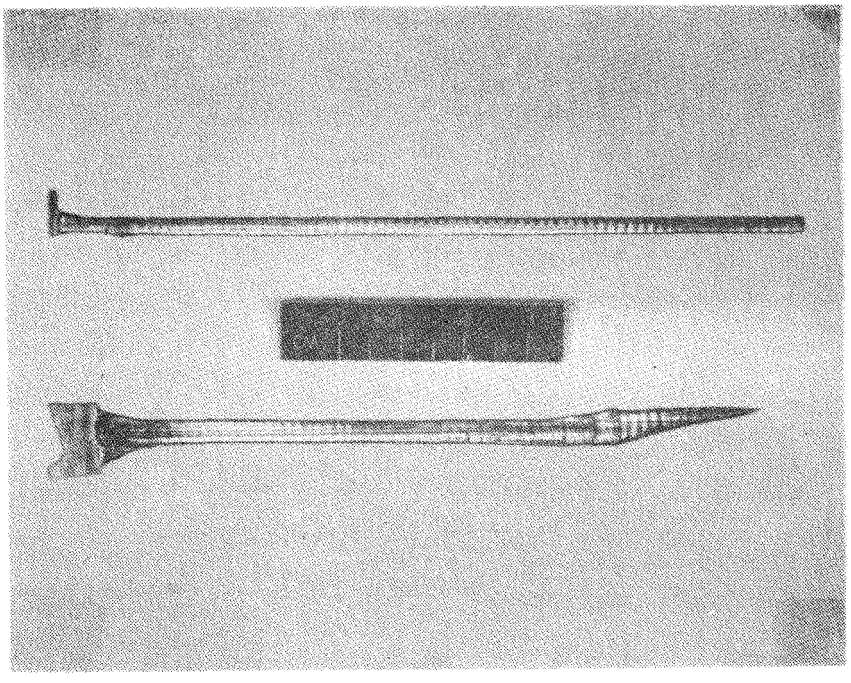

Figure 7. Photograph of silicon ribbons grown with RS-Si_3N_4 die coated with CVD-Si_3N_4.

4. K. M. Kim, G. W. Cullen, S. Berkman, and A. E. Bell, "Silicon Sheet Growth by the Inverted Stepanov Technique," Quarterly Report No. 3, EDRA/JPL/954465-76/3, prepared under Contract No. 954465 for Jet Propulsion Laboratory, Dec. 1976.

The resistivity of the ribbons in Fig. 7 is ∿0.2 ohm-cm. At the present time our ribbon growth and CVD coating system is contaminated with boron. The ribbons contain low-angle grain boundaries parallel to the growth axis (see Section III.C below). The twins are nucleated at the seed-ribbon junction. In the ribbon growth runs the seed was positioned close to or inside the die aperture prior to seeding. The seed tip usually becomes covered with a surface layer, which could have led to the twinning. Seeding procedures are being developed in an attempt to keep the seed clean and improve the crystalline quality. After we established a stable and sustained ribbon growth, experiments were continued with the major emphasis on increasing the ribbon width. The sizes of the die aperture and seed were kept the same as in the earlier experiments. Silicon seeds were of the (110)[11$\bar{2}$] orientation. Thermal trimmers similar to trimmers 1a and 2a described previously [4] were applied. The first trimmer is a pyrolytic graphite (PG) plate with a dog-bone-shaped opening parallel to the die aperture, and the thickness of the PG plate tapers off toward both ends. The second trimmer consisted of a PG plate positioned inside a thin rectangular graphite susceptor. Most growth runs were conducted with the first type of thermal trimmer.

With both types of trimmers, the width of the silicon ribbon continually decreased as the growth proceeded. Figure 8 shows a photograph of a typical silicon ribbon grown with the width instability. The growth direction was downward in the photograph, as indicated by the arrow. Instantaneous s-ℓ growth interface shapes are delineated by the horizontal striations on the ribbon surface (see Fig. 8). The interface shape at the lower end corresponds to the initial seed-ribbon junction. The other two striations represent the interface shapes when the growth was restarted, after the ribbon froze over momentarily to the die and then meniscus was reestablished by an increase in temperature of the growth system. The delineated interface shapes are convex toward the melt, which indicated that the meniscus height at the ribbon end was higher than along the side of the ribbon. Such convex interface shape in the ribbon growth with flat die edge is certainly not suitable for the stable ribbon growth of

constant width, as has been analyzed [5] in detail for the EFG, inverted Stepanov, and inverted EFG process. For the stable growth of wide ribbons, the meniscus height at the ribbon ends should be smaller than along the ribbon side. In other words, the favorable meniscus shape should be slightly concave toward the melt. This originates physically in the fact that one of the two principal radii of curvature of the meniscus undergoes a discontinuous change in the ribbon growth, i.e., from infinity at the ribbon sides to about half the ribbon thickness at the ends. It is of interest to point out that according to an analysis by Surek [5], the stability vs the meniscus height is more favorable in the inverted configuration for both the Stepanov and the EFG processes.

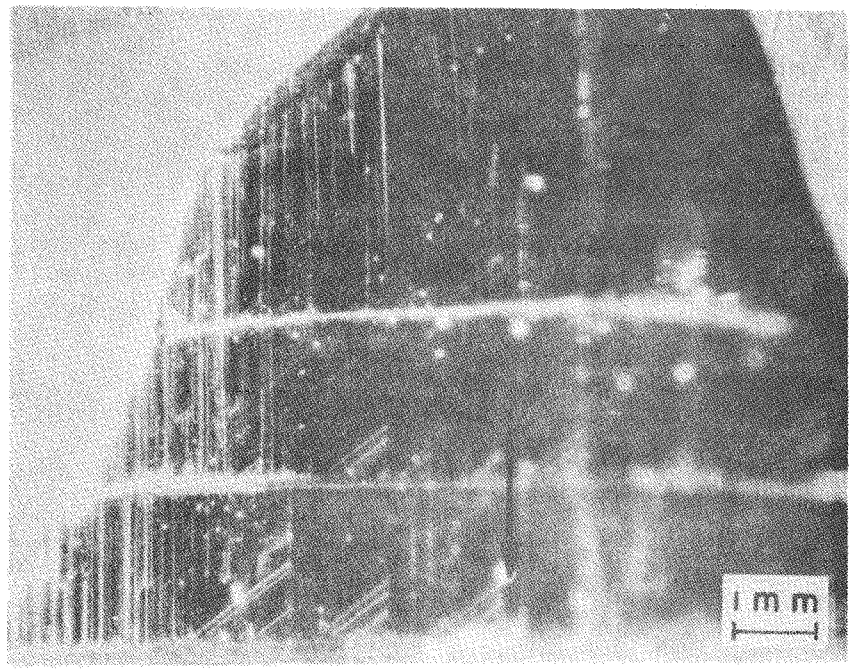

Figure 8. Photograph of a typical silicon ribbon grown with the width instability. The s-ℓ growth interface shapes, convex toward the melt, are revealed by the striations. The growth direction is indicated by the arrow.

5. T. Surek, J. Appl. Phys. 47, 4384 (1976),

The s-ℓ growth interface shape is controlled by both the horizontal temperature distribution in the die aperture prior to seeding and the heat loss through the seed when the meniscus is seeded. In turn, the horizontal temperature profile is controlled by the thermal distribution in the susceptor, melt, and thermal trimmer. In our ribbon growth configuration with the thermal trimmers mentioned above, the horizontal temperature gradient prior to seeding is ∿8°C/cm, the ends being colder than the midpoint. This estimate is based on the observation of the melt freezing inside the die aperture as the set-point of the temperature controller is lowered in small steps corresponding to about 1°C.

Thus, even though the isotherm in the die aperture prior to seeding was concave, a convex interface shape was established after seeding. This is due to the substantial increase of the heat drain at the seeded meniscus, which is calculated to be more than ten times the drain which exists before seeding [6]; the enhanced drain through the seed reverses the isotherm from the concave to the convex shape after seeding.

We believe that the continual narrowing of the ribbon width is caused by the unfavorable convex interface shape. The growth conditions are being modified to flatten the convex isotherm and thus to achieve a wide ribbon growth.

C. X-RAY TOPOGRAPHY OF A SILICON RIBBON GROWN WITH A DIE COATED WITH Si_3N_4

The crystallinity of the silicon ribbon grown with a die coated with CVD-Si_3N_4 was characterized by x-ray diffraction topography. Figure 9 shows a projection topograph taken with Mo radiation using the (111) diffracting planes which are parallel to the growth direction and perpendicular to the surface. Figure 9(a) shows most of the grown ribbon with a portion of the seed at the bottom. The major feature of the ribbon is the series of parallel grains running along the growth direction. Some grains have resolvable dislocation structure; some have sufficient strain to obscure any other detail; and others are misoriented from the Bragg condition for

6. K. M. Kim, G. W. Cullen, S. Berkman, and A. E. Bell, "Silicon Sheet Growth by the Inverted Stepanov Techniques," Quarterly Report No. 1, ERDA/JPL/954465-76/1, prepared under Contract No. 954465 for Jet Propulsion Laboratory, June 1976.

diffraction so as to give no contrast. An enlarged region is shown in Fig. 9(b). The horizontal line near the top of the topograph corresponds to momentary freezing and regrowth. Additional defects are nucleated at this line.

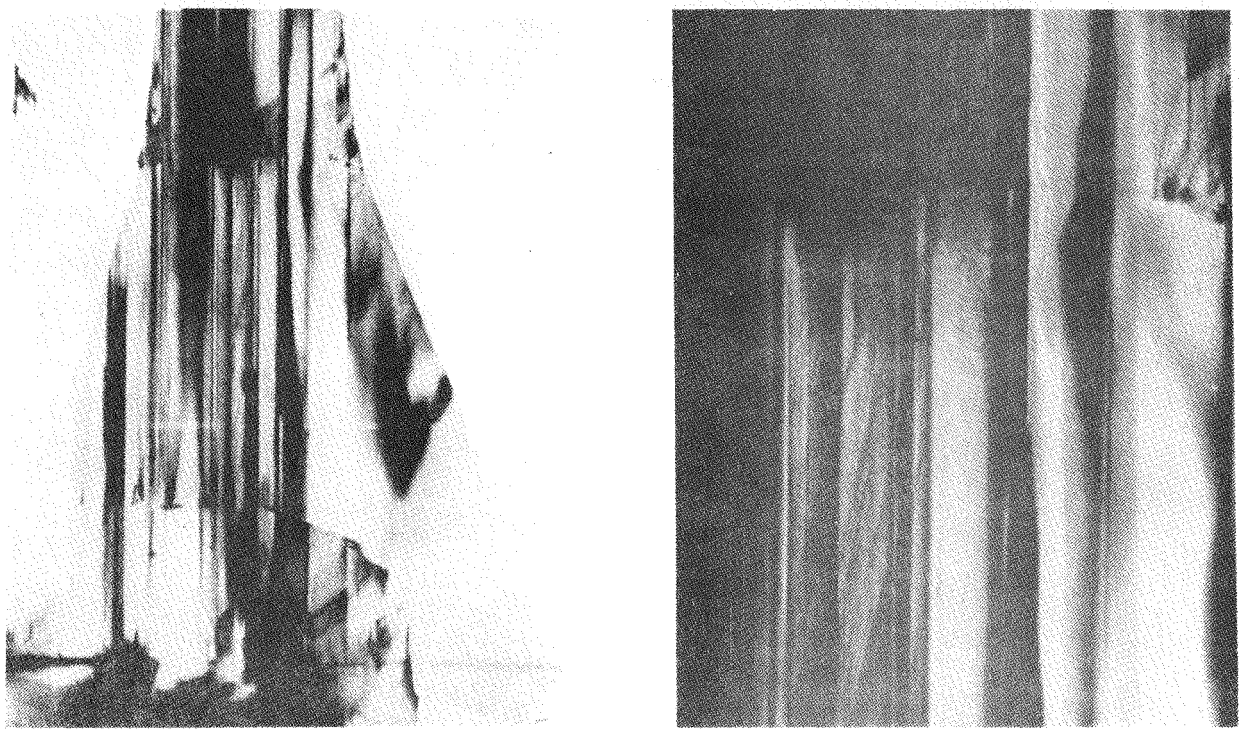

(a) (b)

Figure 9. (111) x-ray projection topograph of a silicon ribbon grown with a die coated with CVD-Si_3N_4. Mo-radiation. (a) Linear defects are revealed in the ribbon. Note the striation at the lower section is the seed/ribbon junction (mag. 5X). (b) A region of the ribbon at higher mag. 16X.

A measure of the misorientation across the several grains was obtained by reorienting the crystal for maximum diffraction intensity at 0.2-mm increments across the crystal. The x-ray beam was only 1.5 mm high for this measurement. Figure 10 shows the relative misorientation as a function of distance across the ribbon. Most of the grains are misoriented only $\pm 0.1°$. A section of the topograph from the region of the ribbon that was observed is shown above the trace.

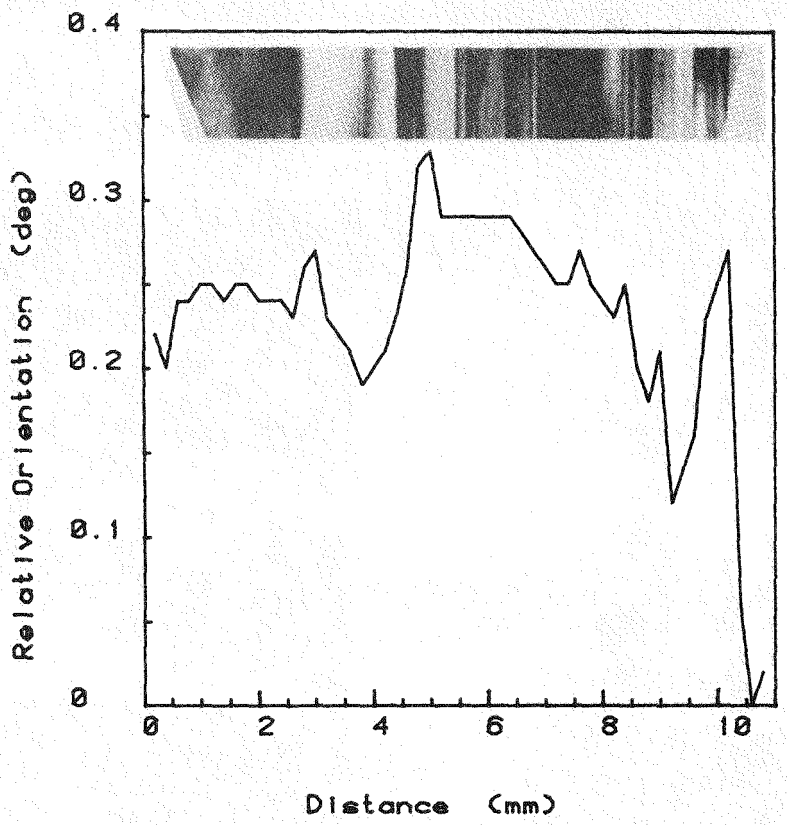

Figure 10. Misorientation across the width of the ribbon shown in Fig. 9. Orientation was measured by repositioning the crystal for maximum intensity at 0.2-mm steps.

D. ASSEMBLY OF MARK II RIBBON GROWTH APPARATUS

The Mark II ribbon puller is being assembled. Figure 11 is a photograph showing the main frame of the puller with the ribbon withdrawal and polysilicon feed mechanism. A high precision lead screw is used for the ribbon pull mechanism, which allows misalignment of only 12 μm per 30-cm stroke. The growth chamber consisting of a rectangular fused silica tube, rf coil, and other parts will be added.

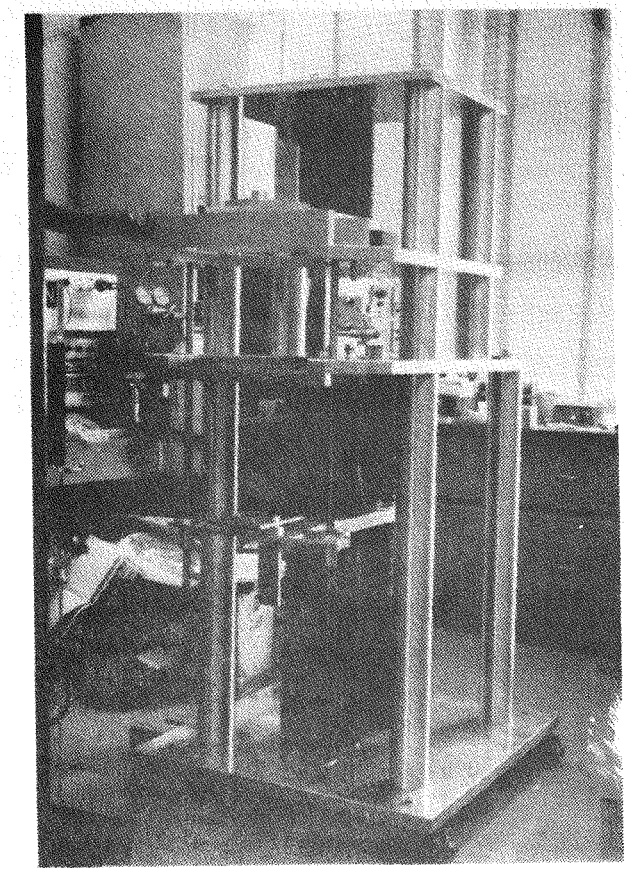

Figure 11. Photograph of the Mark II ribbon growth apparatus being assembled.

SECTION IV

CONCLUSIONS AND FUTURE PLANS

Preliminary evaluation of the reactivity of the molten silicon with the CVD-Si_3N_4 and CVD-SiO_xN_y indicates that these materials are considerably more resistant to reaction with and/or dissolution in silicon than other materials examined to date. Of the various substrates examined, the RS-Si_3N_4 is the most favored. Graphite (such as UT-8) may prove to be a suitable substrate material. The effort to find the appropriate substrate material for the CVD-Si_3N_4 and Si_3N_4 coatings will continue. With the better substrates, the physical and chemical integrity of the coatings will be evaluated.

Stable growth of narrow ribbons has been achieved by using dies coated with CVD-Si_3N_4. In a number of growth runs to establish conditions for the growth of wide ribbons, the width decreased continually as the ribbon growth proceeded. The width instability is due to the convex isotherm during seeding and ribbon growth. Thermal conditions of the ribbon growth arrangement are being modified to flatten the currently observed convex interface shape in an effort to achieve a wide ribbon growth. The modifications include the use of a curved die, proper thermal trimming to enhance the heat loss at the ends, and melt containment away from the ends. As the stable growth of wide ribbons becomes established, more efforts will be made to improve the crystalline quality and the impurity level.

The assembly of the Mark II puller is on schedule, and will be finished soon.

REFERENCES

1. A. V. Stepanov et al., Bull. Acad. Sci. USSR, Phys. Series 33, 1826 (1969)
2. J. C. Schwartz, T. Surek, and B. Chalmers, J. Electronic Mat. 4, 255 (1975); H. E. Bates, F. H. Cooks, and A. I. Mlaxsky, "Thick Film Silicon Growth Technique," NAS-100/JPL-953365, First Quarterly Progress Report, July 1972.
3. T. F. Ciszek, Mat. Res. Bull. 7, 731 (1972).
4. K. M. Kim, C. W. Cullen, S. Berkman, and A. E. Bell, "Silicon Sheet Growth by the Inverted Stepanov Technique," Quarterly Report No. 3, ERDA/JPL/954465-76/3, prepared under Contract No. 954465 for Jet Propulsion Laboratory, Dec. 1976.
5. T. Surek, J. Appl. Phys. 47, 4384 (1976).
6. K. M. Kim, G. W. Cullen, S. Berkman, and A. E. Bell, "Silicon Sheet Growth by the Inverted Stepanov Technique," Quarterly Report No. 1, ERDA/JPL/954465-76/1, prepared under Contract No. 954465 for Jet Propulsion Laboratory, June 1976.
7. K. M. Kim, G. W. Cullen, S. Berkman, and A. E. Bell, "Silicon Sheet Growth by the Inverted Stepanov Technique," Quarterly Report No. 2 ERDA/JPL/954465-76/2, prepared under Contract No. 954465 for Jet Propulsion Laboratory, September 1976.

APPENDIX A

NEW TECHNOLOGY

It has been found that CVD-SiO_xN_y is relatively unreactive in contact with molten silicon. Thin films of the SiO_xN_y may be applied to various refractory substrate materials, such as RS-Si_3N_4. The composite structure appears to be a promising material in applications which involve the containment of molten silicon.

It is to be recognized that the conception and reduction to practice of the chemically vapor deposited silicon nitride and silicon oxynitride were carried out under RCA funding and predate the inclusion of these materials in this Contract effort (see JPL Technical Direction Memorandum dated 12/8/76) and, therefore, are not "subject inventions" under the Contract.

APPENDIX B

STEPANOV GROWTH PROGRAM PLAN*

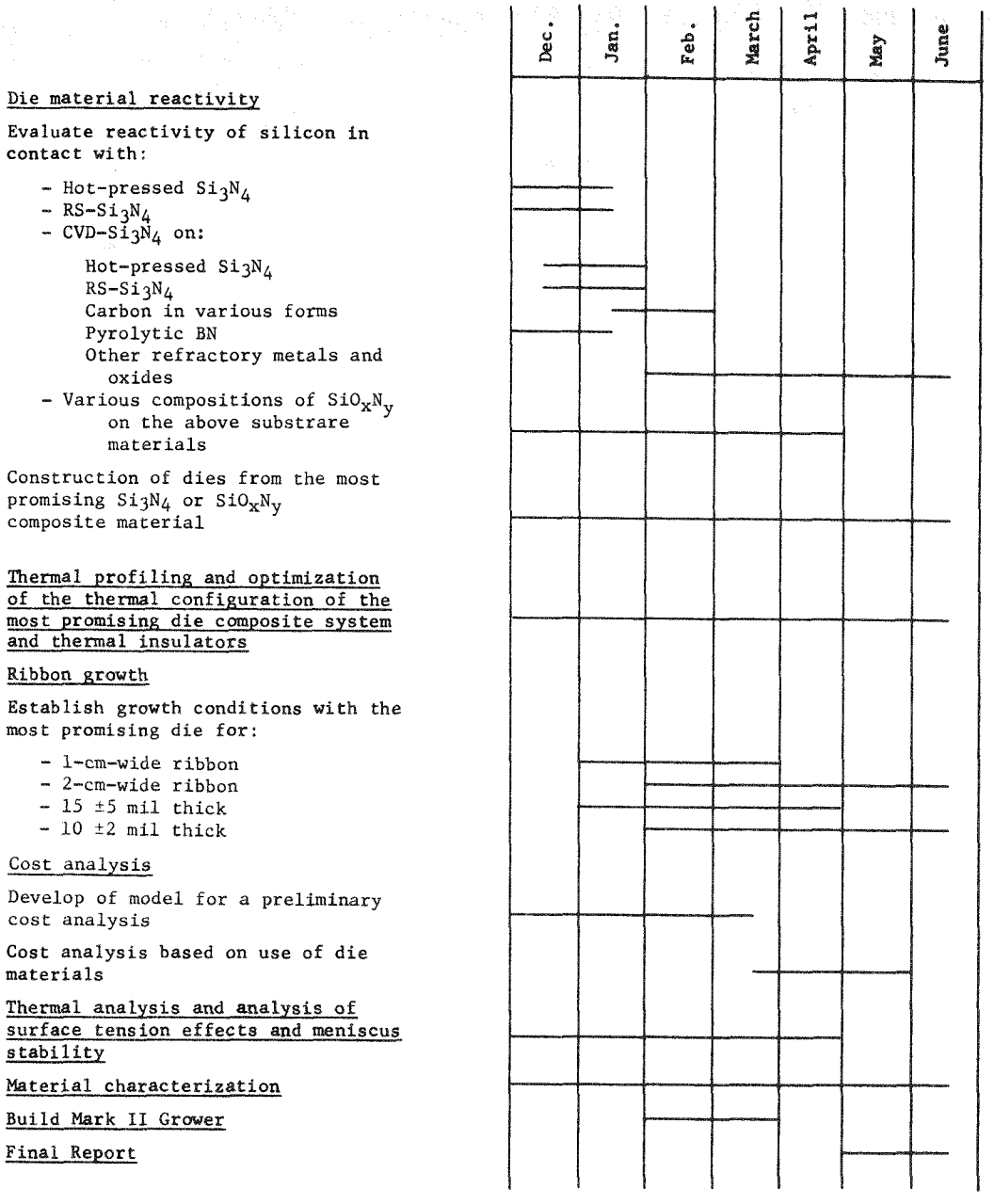

*This is a revised program plan based on the adoption of new composite dies coated with CVD-Si_3N_4 and CVD-SiO_xN_y.

APPENDIX C

MANHOURS AND COSTS

At the end of the third quarterly period, manhours were 2828 and cost plus fixed fee was $100,317. Manhours for January and February were 529 and cost plus fee was $23,565. Manhours for March are estimated to be 375 and cost plus fixed fee to be $13,000. Fourth quarter manhours are estimated to be 904 and cost plus fixed fee to be $36,565. Cumulative manhours and cost plus fixed fee are estimated to be 3732 and $136,882, respectively. See Figs. C-1 and C-2.

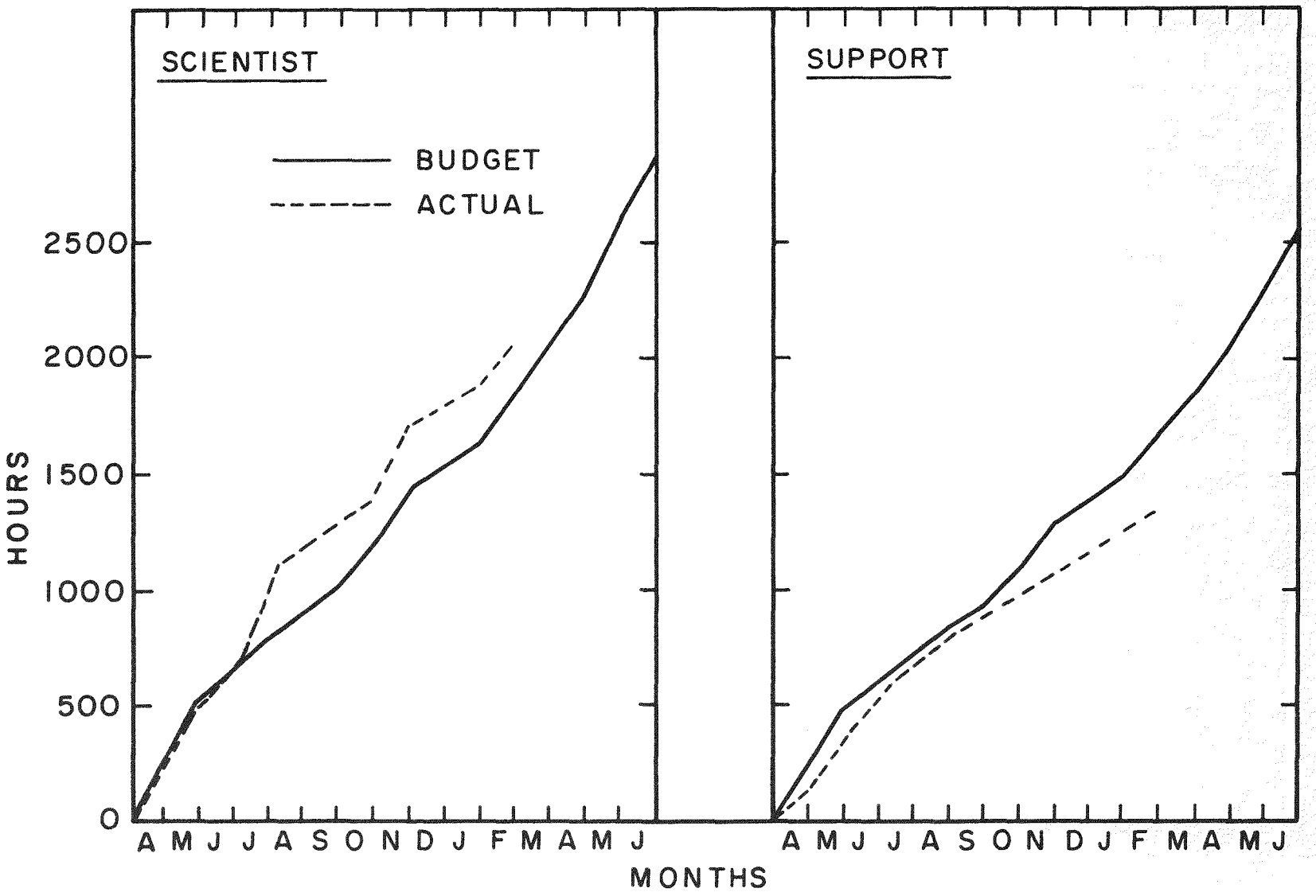

Figure C-1. Manhour chart.

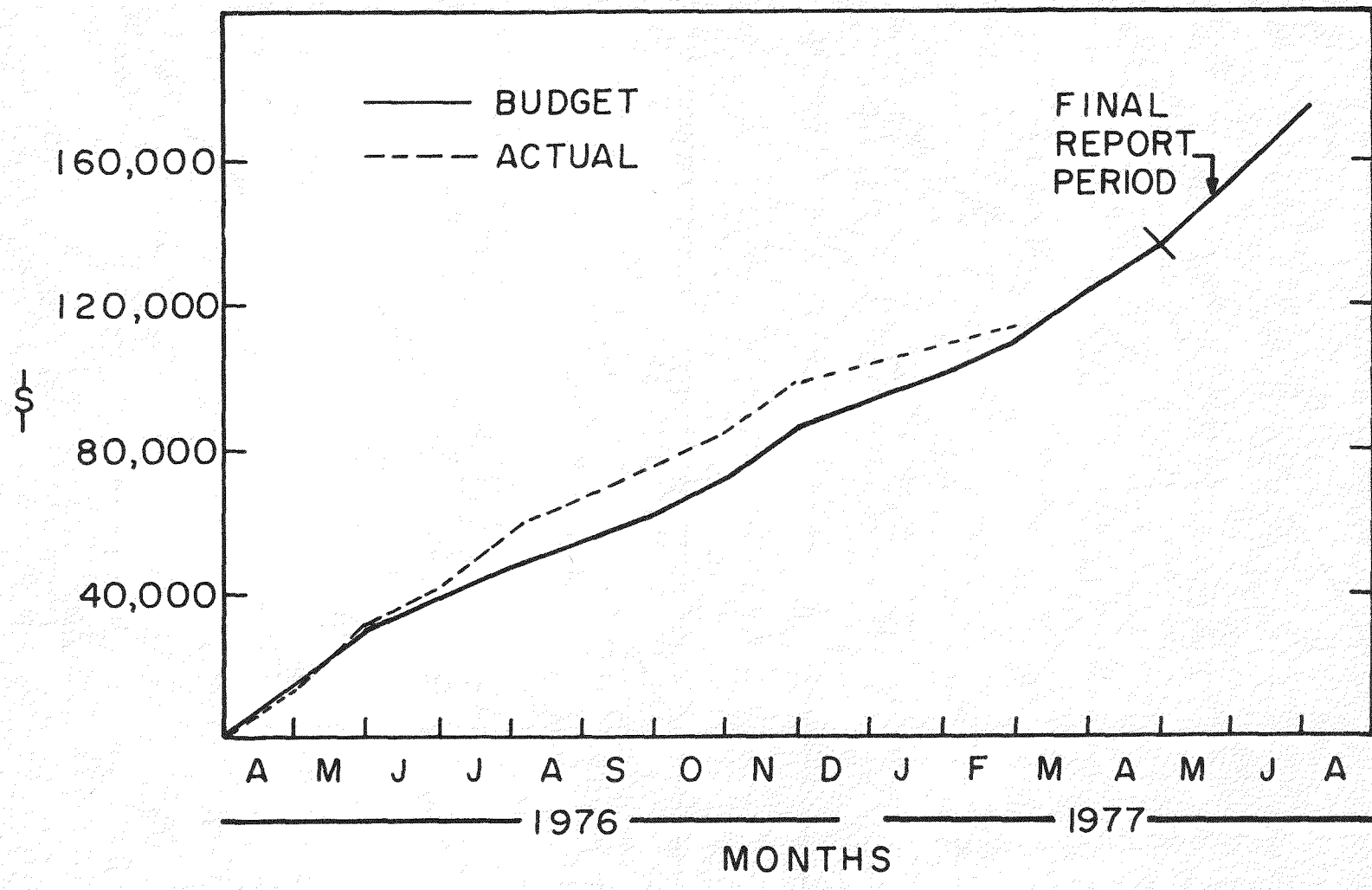

Figure C-2. Cost chart.

☆U.S. GOVERNMENT PRINTING OFFICE: 1977-740-